



Comparative Assessment of Solar Dryer with Thermal Energy Storage System and Heat Pump Dryer in Terms of Performance Parameters and Food Analysis

Özlem Timurtas^a , Gökhan Gürlek^{b*} 

^aGraduate School of Natural and Applied Science, Ege University, Izmir, TÜRKİYE

^bFaculty of Engineering, Department of Mechanical Engineering, Ege University, Izmir, TÜRKİYE

ARTICLE INFO

Research Article

Corresponding Author: Gökhan Gürlek, E-mail: gokhan.gurlek@ege.edu.tr

Received: 15 November 2023 / Revised: 18 February 2024 / Accepted: 22 February 2024 / Online: 23 July 2024

Cite this article

Timurtas Ö, Gürlek G (2024). Comparative Assessment of Solar Dryer with Thermal Energy Storage System and Heat Pump Dryer in Terms of Performance Parameters and Food Analysis. *Journal of Agricultural Sciences (Tarim Bilimleri Dergisi)*, 30(3):594-605. DOI: 10.15832/ankutbd.1391447

ABSTRACT

Striving for the highest quality food product in the shortest time with the least energy expenditure is the cornerstone of the food drying process. Furthermore, the geometric properties of the product significantly influence the efficiency of the drying process. Therefore, in this study, peach slices of three different thicknesses were dried in three different dryer types. The drying of peaches was carried out using a solar energy drying system, a thermal energy storage solar dryer, and a dryer with a heat pump. The drying performances of peach slices of three different thicknesses were investigated. Moisture extraction rates (MER), specific moisture extraction rates (SMER), and specific energy consumption

(SEC), which relate to the amount of removed moisture and the amount of consumed energy at the end of the drying studies, were calculated. Food analyses, such as moisture content, color, texture, and water activity were performed. Considering the amount of energy consumed, it is seen that the heat pump system consumes more energy than the solar energy system. In addition, by using the heat storage system, the drying time is shortened, and the energy consumption is reduced. A decrease in SEC values was observed with the activation of the heat storage solar dryer.

Keywords: Solar assisted dryer, Basalt stone, Thermal energy storage, Heat pump dryer

1. Introduction

Since drying is a highly energy-demanding process, various drying systems have been developed to increase energy efficiency and reduce energy costs. Solar dryers are systems that provide higher energy savings compared to other drying technologies. However, the great disadvantage of these systems is that their operation is restricted to sunlight. Energy storage methods have been developed to store solar energy as heat energy to continue drying even without the sun. When there is little or no sunlight, this stored energy is converted into usable energy. Thus, while shortening the total drying time, economical and hygienic drying is provided (Atalay 2019). Considering these circumstances, the significance of energy storage mediums in industrial drying processes is steadily growing. Many studies on solar-powered dryers and thermal storage systems have been carried out. While agricultural products and seafood were dried by Fudholi et al., within the scope of solar drying studies (Fudholi et al. 2014), drying models were obtained by drying mint leaves in another study (Akpınar 2010). Pepper (Akin et al. 2014), tomato (Gürlek et al. 2009), bitter melon slices (Vijayan et al. 2020), apple, and mint (Şevik et al. 2019) were dried using solar air collectors. The drying of asparagus roots was examined in a distinct study by Kohli et al., using four different drying methods at 40, 50, 60, and 70 °C in sun drying, tray drying, fluidized bed drying, and vacuum drying (Kohli et al. 2021).

Energy storage systems offer a solution to the discontinuity problem encountered in renewable energy applications. Thus, the operating costs of the system used are reduced (Gunerhan & Hepbasli 2005). Heat storage materials are expected to have certain thermo-physical qualities such as high thermal conductivity and heat storage capacity. Many studies have been done on the capacity of materials to store thermal energy. As thermal energy storage (TES) material, sand, rock, aluminium (Natarajan et al. 2017), pebble (Atalay 2020; Chaouch et al. 2018), paraffin wax (Atalay 2020), concrete, sand, and rock bed (Ayyappan et al. 2016) were used. Apricot (Baniasadi et al. 2017), apricot, onion, pea (Rehman et al. 2023), radish, pepper, mushroom (Qiu et al. 2016), wheat seeds (Singh et al. 2022), and crop (Abubakar et al. 2018) drying studies were also dried using heat storage materials.

Since the drying process is an intense energy consuming process, the use of heat pumps has emerged as an alternative in drying operations. It is stated that energy consumption will decrease with the increase in efficiency in heat pump systems used

in drying applications (Goh et al. 2011). Evaluation of the physical attributes of heat-pump-dried food reveals its consistently superior quality compared to conventionally dried counterparts. According to the research with tray dryer, microwave dryer, heat pump dryer and freeze dryer conducted by Baysal et al. (2015), the heat pump dryer had the lowest energy consumption and the highest MER and SMER values (Baysal et al. 2015). Also, sliced apple (Aktaş et al. 2019), tomato (Queiroz et al. 2004) cereals (Liu et al. 2019), sliced radishes (Lee & Kim 2009), plums (Hepbasli et al. 2010), cotton cloth (Ganjehsarabi et al. 2014), and apple (Gürlek et al. 2015) drying studies were carried out using a dryer with a heat pump.

The drying method and drying system affect the product quality. Properties of the dried product, such as color, odor, final moisture content, water activity value, aroma, nutritional value, and content of harmful substances such as aflatoxin, determine the quality of the product. Exposing the products to high temperatures during the drying process degrades the quality. The process temperature can be lowered to increase product quality, attention should be paid to the increase in drying time and drying costs (Nindo et al. 2003). Different drying processes affect product quality directly. For example, long exposure to the hot air generated by electrical resistance decreases the quality of the products. On the other hand, high operating costs also arise in the freeze-drying process where high-quality products are obtained (Huang et al. 2011). It was determined that dried apple slices produced by freeze drying and microwave methods are of higher quality compared to those produced by tray and heat pump drying methods (Baysal et al. 2015). In another study, kiwi fruit was air-dried at four different temperatures and its drying properties were determined (Orikasa et al. 2008). Using a combined convection-microwave dryer, Kesbi et al. studied the drying of lemon slices. Measurements of L^* , a^* , b^* , a total color difference, chroma, and rehydration capability were used to assess the dried lemon slices' quality (Mirzabeigi Kesbi et al. 2016). In their study to dry Brussels sprouts, Nakilcioğlu-Taş and Ötleş determined that a^* , ΔE and browning index increased with increasing microwave output power during drying (Nakilcioğlu-Taş & Ötleş 2018). Polat et al. carried out drying studies of peach puree using microwave dryer, convective dryer, and combined convective-pulsed microwave dryer. They examined the drying curves, color, pH and microstructure of the dried products (Polat et al. 2021).

Inspired by the fact that heat pump dryers and solar dryers are cheaper than other dryers, we hypothesize that low energy consumption and high-quality drying can be realized in a shorter drying time by using three different types of dryers: solar energy drying systems (SEDS), thermal energy storage drying systems (TESDS), and heat pump drying systems (HPDS). The results obtained from the solar-powered dryer when the storage unit is active, and passive were compared with the results of the experiments made with the dryer with a heat pump at the same temperature. In SEDS, drying was carried out during the hours of solar radiation, while continuous drying was carried out in TESDS and HPDS. The results include an evaluation of the positive effects of the thermal energy storage (TES) system on system performance, energy consumption, and drying time. Additionally, the study examines the quality characteristics of the dry products obtained through the drying process in different dryers. Thus, besides the amount of energy consumed, quality criteria were also evaluated. It is expected that the effect of the TES system on the drying time, the performance parameters of three different drying systems, and the product quality characteristics discussed in the study will contribute significantly to the literature.

2. Material and Methods

2.1. Dried material

The peach was used in the drying study. Peach (*Prunus Persica*) fruit is a downy fruit from the Rosaceae family of the order Rosales and is mostly grown in tropical-subtropical regions in the world. It contains vitamins A and C, fiber, potassium minerals, and phytochemical compounds such as anthocyanin, total phenol, and flavonoid (Saidani et al. 2017).

2.2. TES material

Unlike the literature (Kant et al. 2016) that uses many energy storage materials in solar drying systems, basalt stone was used as an energy storage material in this study. Basalt, along with granite, is one of the two most common rocks in nature. It is an extrusive rock with fine grains and contains more iron and magnesium with respect to granite. It usually consists of minerals such as olivine, pyroxene, and feldspar. Basalt has a hard, dark, and dense texture. Being a hard material provides superior abrasion resistance in basalt. It was formed by the solidification of magma and its melting point temperature is above 1050 °C. It has a density between 2800 and 2900 kg/m³. Thermo-physical properties related to basalt stone are shown in Table 1 (Gunerhan & Hepbasli 2005; Hartlieb et al. 2016; Nahhas et al. 2019).

Table 1-Physical properties of basalt rocks (Hartlieb et al. 2016).

<i>Physical properties of basalt stone</i>	
Density (kg/m ³)	2870
Specific Heat Capacity (J/kg K)	898
Thermal Capacity (MJ/m ³ K)	2.58
Diffusivity (mm ² /s)	0.79
Thermal Conductivity (W/mK)	1.55

2.3. Experimental setup of solar dryer With/Without TES system

Three types of dryers were used for experimental studies: SEDS, TESDS, and HPDS. The designed and produced solar dryer with a TES unit is shown schematically in Figure 1-a. The system consists of basic elements such as solar air collectors (2), drying cabinet (1), perforated shelves to accelerate the heat transfer mechanism (3), fans (5,6), waste heat recovery unit (7), and TES unit (14). The TES unit consists of three solar air collectors (8), fans (11,12), and basalt stone (13). In addition, the crossflow heat exchanger (7) installed in the drying system allows the waste heat to be recovered at a certain rate. The drying cabinet is surrounded by insulation material (0.030 W/mK) with a low heat conduction coefficient to prevent heat loss. The five solar air collectors used in the system are made of double-layer polycarbonate cover material and polystyrene insulation material surrounding the main body.

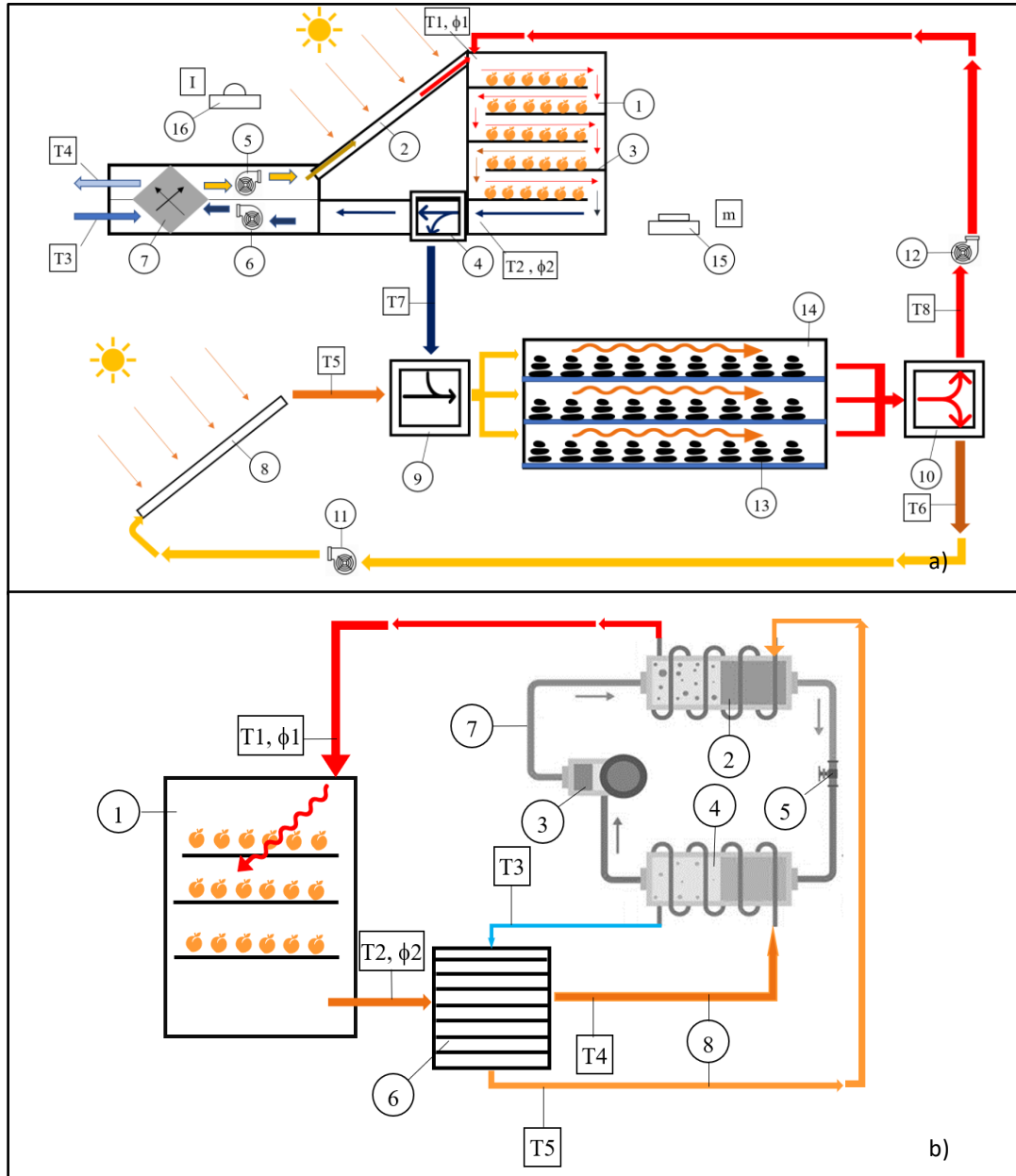


Figure 1-Schematic representations a) the solar assisted thermal energy storage dryer, b) the dryer with a heat pump

Fresh air taken from the outside is heated by passing through solar energy collectors (2). The air, whose temperature is brought to drying temperature, is contacted with the product to be dried in the drying cabinet (1). The air, whose temperature decreases, and humidity increases, leaves the drying cabin, and is sent to the crossflow heat exchanger (7) in the waste heat recovery unit. The energy in the air leaving the drying cabin is transferred to the fresh air taken from outside through this heat recovery exchanger. Thus, the temperature of the fresh air is slightly increased before it enters the solar energy collector, and heat recovery is achieved. During daylight hours, the energy storage unit (14) works in parallel with the drying unit but independently of each other. In the three solar energy collectors (8) in this system, the heated air enters the energy storage cabinet (13). The air transfers

its energy to the basalt stones and is sent to the collectors with a reduced temperature. The energy obtained during the hours of sunlight is stored in basalt stones. When the solar radiation values are insufficient for the drying process, the airflow direction is changed with dampers (4,9,10). Thus, the low-temperature air leaving the drying cabinet enters the energy storage cabin via dampers (4, 9). Drying air temperature increases with the stored energy it receives from basalt stones. The drying air, whose temperature increases, is sent back to the drying cabinet by the damper (10). Thus, the drying process is carried out continuously during the hours when there is no sunlight.

During the drying process, anemometer was used for air velocity measurement at the entrance of the drying cabinet and similarly pyranometer was used for solar radiation (I) measurement in the system. The product mass (m) loss was recorded at 30 minutes intervals by means of a precision balance. The humidity of the drying air was measured at the entrance and exit of the drying cabinet. Drying cabinet inlet and outlet temperatures (T1, T2), waste heat recovery unit inlet and outlet air temperatures (T3, T4), inlet and outlet air temperatures (T7, T8) when the energy storage system is active and energy storage unit inlet and outlet air temperatures (T5, T6) were measured every five minutes.

2.4. Experimental setup of the HPDS

Another system used is the HPDS shown schematically in Figure 1-b. The heat pump unit, drying cabinet (1), drying air ducts (8), and heat recovery unit (6) are the main components of the HPDS. The heat pump unit, on the other hand, consists of the compressor (3), condenser (2), evaporator (4), refrigerant channel (7), and expansion valve (5).

The drying cabinet is constructed from panels that are 8 cm thick and have polyurethane insulation. The shelf arrangement is made gradually and the passage of the drying air through the entire product surface is provided. The shelves are made of perforated steel wires for maximum contact of the drying air with the product. Air ducts are made of 0.6 mm thick galvanized sheet material. Insulation is made to prevent heat loss from air ducts. The heat pump unit used in the drying system allows drying to a maximum of 55 °C.

The HPDS is a two-fluid system. R404 refrigerant is used as the fluid. The refrigerant evaporated by the heat drawn from the drying air in the evaporator part of the heat pump unit is compressed up to the condenser pressure with the compressor. In the condenser, the thermal energy within the refrigerant transfers to the drying air, and the temperature of the drying air increases up to the drying temperature. The temperature of the refrigerant decreases a little after transferring its energy to the drying air. The refrigerant leaving the condenser at a relatively low temperature and high pressure is throttled in the expansion valve until the evaporator pressure. Thus, the cycle of the refrigerant is completed. The drying air enters the drying cabinet after being heated in the condenser. After the drying process, it comes to the heat exchanger with a decrease in temperature and an increase in moisture. Here, the temperature of the low temperature drying air leaving the evaporator is slightly increased before it enters the condenser. Thus, system efficiency is increased by preheating.

Temperature values (T2, T3, T4, T5) from the inputs and outputs of the waste heat recovery unit and the temperature (T1, T2) and humidity values (ϕ_1 , ϕ_2) at the entrance and exit of the drying cabin were measured and recorded. Sizing information for both drying systems is shown in Table 2.

Table 2-Dimensions and capacities of dryer equipment's

<i>Dryer systems dimension and capacity</i>	
<i>Solar dryer with thermal energy storage system</i>	
Drying Cabin (length x width x height)	2.3 m x 2.3 m x 2.3 m
Solar Air Collector (length x width)	2 m x 1 m
Distance Between Perforated Shelves	0.4 m
Waste Heat Recovery Unit (length x width x height)	1.1 m x 0.4 m x 0.4 m
Thermal Energy Storage System (length x width x height)	2 m x 1 m x 1 m
<i>Heat pump dryer</i>	
Compressor	1300 W
Condenser	4800 W
Evaporator	3500 W
Drying cabin (length x width x height)	0.86 m x 0.86 m x 1.20 m
Air Vent (length x width)	0.40 m x 0.20 m
Perforated Shelves (length x width x height)	0.70 m x 0.70 m x 0.02 m

2.4. Determination of energy efficiency in drying systems

The efficiency of drying systems was assessed using moisture extraction rates (MER), specific moisture extraction rates (SMER), and specific energy consumption (SEC). SMER is defined as kilograms of moisture removed (MoR) per kilowatt-hour of energy

consumed during drying (EC). Consumed energy relates to the total power of the dryer, including the power of the fan and electrical equipment. The amount of moisture evaporating in drying time (DT), or MER, is a indicator of drier capacity. The total energy needed to remove one kilogram of water is known as SEC, which is the opposite of SMER (Baysal et al., 2015). SMER, MER, and SEC values are calculated with the following equations respectively.

$$SMER = \frac{MoR}{EC}, \left(\frac{kg}{kW} \right) \quad (1)$$

$$MER = \frac{MoR}{DT}, \left(\frac{kg}{h} \right) \quad (2)$$

$$SEC = \frac{EC}{MoR}, \left(\frac{kWh}{kg} \right) \quad (3)$$

2.5. Food analysis of dried products

In this study, dried peach slices of different thicknesses were subjected to various food analyses such as moisture, water activity, color, and texture profile.

2.6. Determination of moisture content

The moisture content determination of dried peach slices was made in a vacuum oven (Wisd, WiseVen, Germany). Three grams of samples were kept in a vacuum oven at 67 °C until they reached constant weight in petri dishes. The amount of moisture was calculated as a percentage based on the dry base.

2.7. Determination of water activity

A water activity measuring instrument (Testo AG 400) with an accuracy of ± 0.001 was used to calculate the water activity value, which is defined as the ratio of the product's equilibrium vapor pressure to pure water's equilibrium vapor pressure at the same temperature. To determine the water activity (aw), approximately 3-4 g of sliced peach sample was placed into the instrument's sealed chamber made of stainless steel. When there is a change of less than 0.001 in the water activity value, it is assumed that the system has reached the balance, and the water activity value is read from the indicator of the device. Fruits with an aw value below 0.7 were considered dried fruit (Bourdoux et al. 2016). The basis of the measuring device is to calculate the water activity value of the product using the following equation:

$$a_w = \frac{P}{P_0} \quad (4)$$

Where; P and P₀ denote the vapor pressure of the water in the product and the vapor pressure of pure water, respectively.

2.8. Color determination

A Hunter Lab Color Flex (CFLX 45-2) was used to measure the color values of dried peach slices. The values of the color parameters L*, a*, and b* were established. The product's brightness, redness, and yellowness are indicated by the values L*, a*, and b* respectively. After standardization, fresh and dried product a*, L*, and b* values were determined. The subscript "ref" states the color of the fresh peach slices accepted as a reference in equation 5 and equation 6. The L* value takes values starting from 0 for dark colors and continuing up to 100 for light colors. Total color difference (ΔE) and color intensity (chroma, ΔC) are calculated according to the following equations respectively. Total color difference, a calorimetric statistic that combines a*, b*, and L* is frequently used to describe the color change in foods during drying processing. Chroma value refers to the saturation degree of the color and changes in proportion to the strength of the color (Baysal et al. 2015).

$$\Delta E = \sqrt{(L^* - L^*_{ref})^2 + (a^* - a^*_{ref})^2 + (b^* - b^*_{ref})^2} \quad (5)$$

$$\Delta C = \sqrt{(a^* - a^*_{ref})^2 + (b^* - b^*_{ref})^2} \quad (6)$$

2.9. Tissue profile (shearing) analysis

Tissue profile analyzes of dried peach slices were performed using TAXT Express tissue analyzer (Stable Microsystems, Surrey, UK) and shear forces were calculated.

2.10. Statistical analysis

Statistical analysis was applied to results from the triplicate trials. In the statistical evaluation of food analysis results, the differences between samples were determined using one-way ANOVA analysis. Tukey test was used to determine significant differences at $P < 0.05$.

2.11. Experimental drying processes

Peaches were sliced in thicknesses of 3, 5, and 10 mm using a slicing machine. The sliced peaches were dried in three drying options (SEDS, TESDS, HPDS) and the data during drying were examined. Experiments have been started by using solar energy-assisted TES system. Measurements were taken at the determined points in the system. Data was collected at regular intervals to monitor the drying process of peach slices. Solar radiation levels were measured every 10 minutes, the mass loss of the peach slices was recorded every 30 minutes, and temperature and humidity values were captured every 5 minutes. Temperature and humidity were measured and recorded at various locations throughout the dryer with heat pump. The mass loss in peach products during drying was determined by regularly weighing the product. According to the data obtained during the studies, temperature and humidity distributions, air velocity changes, solar radiation values during the day, drying rate, and moisture content curves were analyzed.

In SEDS, drying was carried out during the hours when solar radiation was present, while continuous drying was carried out in TESDS and HPDS. Thus, total drying times for different drying options were determined. Based on the energy consumed for drying, SMER, MER, and SEC values were compared. The quality properties of the dry products were obtained. Thus, besides the amount of energy consumed, quality criteria were also evaluated.

3. Results and Discussion

At first, peach slices of 3-, 5-, and 10-mm thickness were dried in SEDS. Figure 2 shows the radiation values of these drying processes and the inlet - outlet air temperatures of the drying chamber. In all three experiments, the irradiance values were around 1000 W/m^2 at noon. Sudden changes in radiation values in the 5 mm peach drying study can be explained by the cloudiness. In all drying studies, the difference between the temperature of the inlet air (T1) and the temperature of the outlet air (T2) is maximum at noon and is the lowest in the morning and evening hours. The ambient air temperature (T3) varied in the range of 25-30 °C throughout the experiments. The data obtained revealed that the experiments were carried out in similar weather conditions. Each experiment was started at 11:00 am and continued until the products were dry. 3 mm peach slices were dried until 17:00, 5 mm peach slices were dried until 19:00, and the drying process of 10 mm peach slices was finished on the second day. 3 mm slices dried in 6 hours, 5 mm slices dried in 8 hours, and 10 mm slices dried in 14 hours are shown in Figure 2.

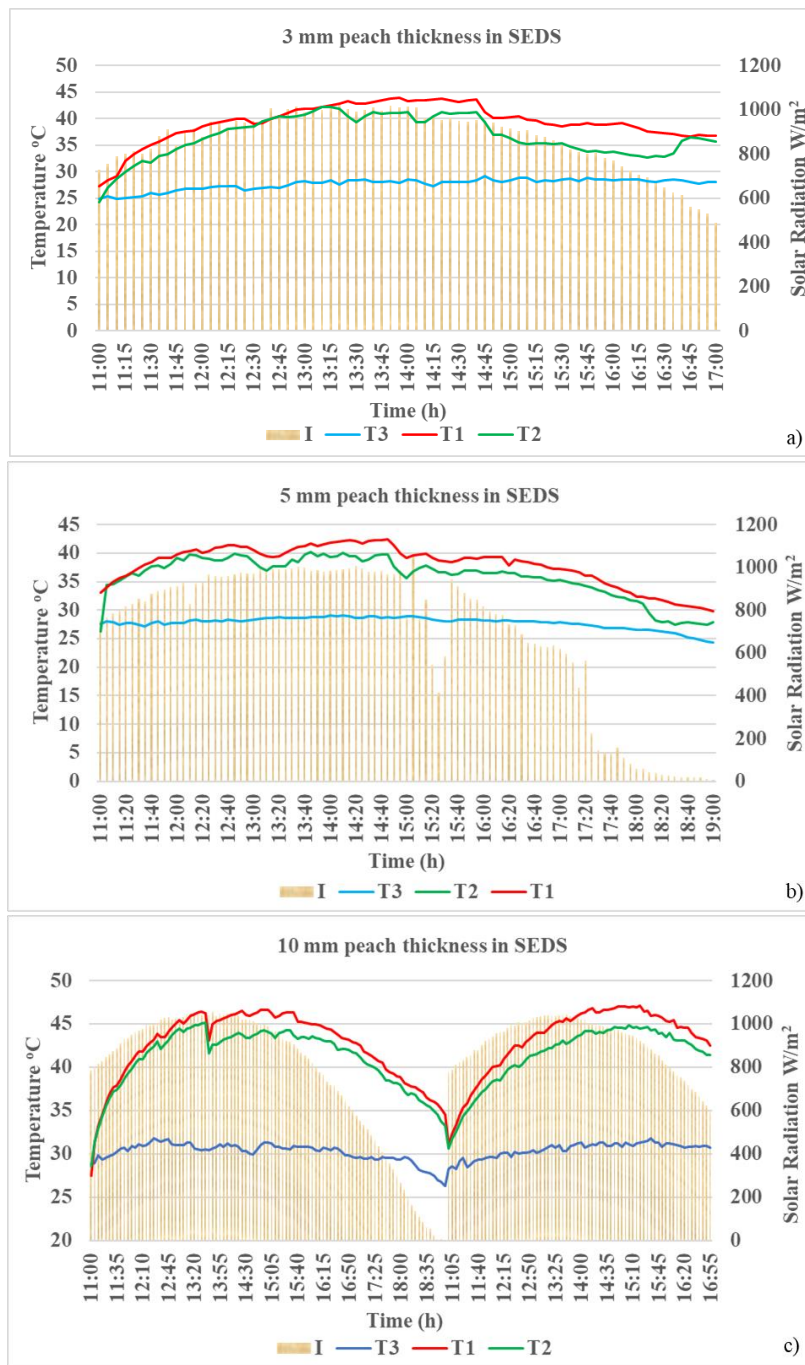


Figure 2-Solar radiation and drying temperatures for different peach thicknesses a)3 mm, b)5 mm, c)10 mm in SEDS

It was observed that as the peach thickness increased, the drying times were prolonged and even delayed to the second day. Reducing drying times is important for system performance and costs. For this reason, new studies have been carried out by including the TES unit using basalt stone in the drying system. Firstly, drying was applied to 3 mm thick peach slices. The drying was started at 11:00 and was completed at 17:00. During the experiment, there was no need to activate the TES unit by opening the dampers during the drying of 3 mm-thick products.

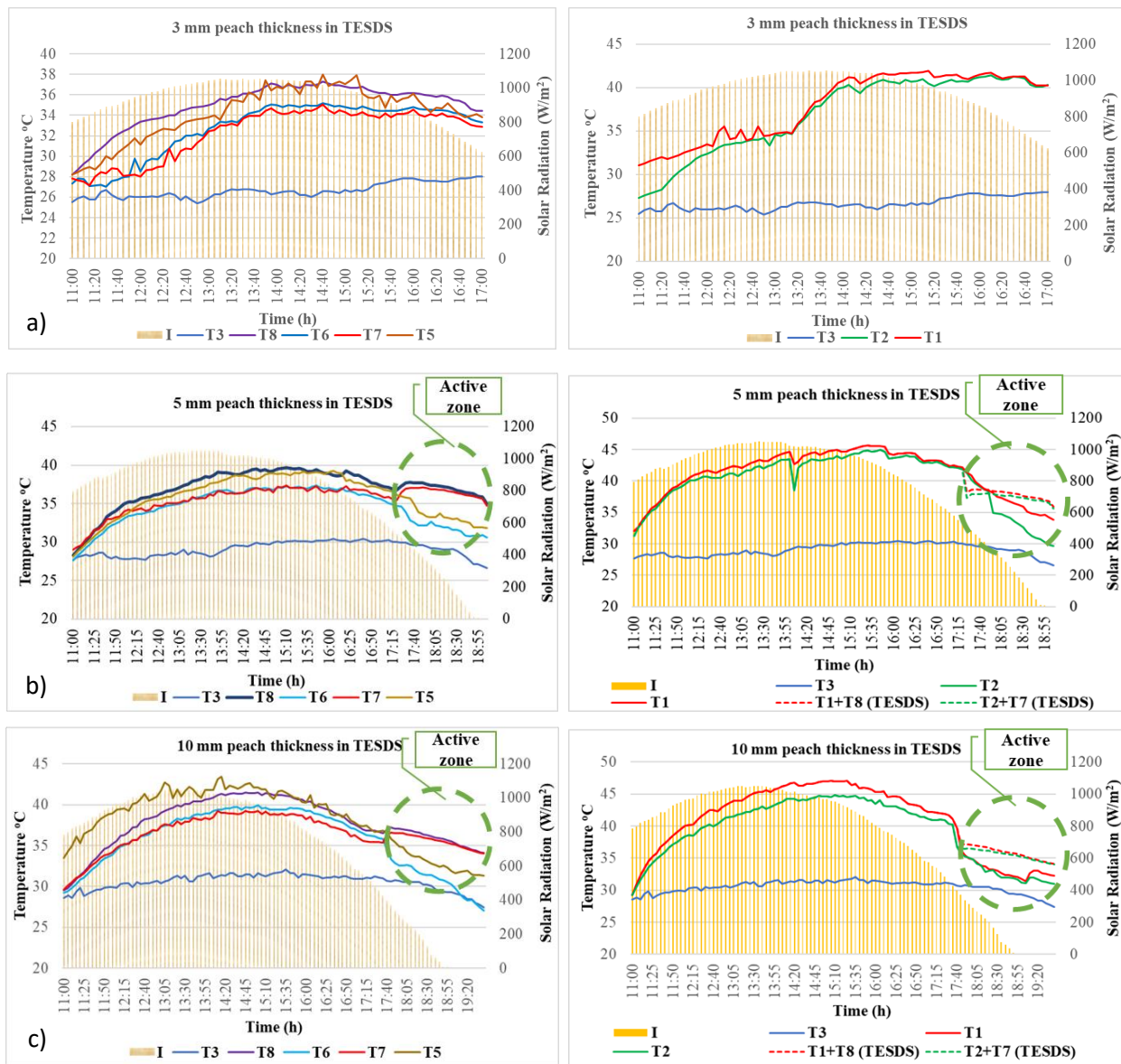


Figure 3-Solar radiation and drying temperatures for a) 3 mm peach in TESDS, b)5 mm peach in TESDS, c) 10 mm peach in TESDS

In Figure 3-a, daily solar radiation values (I), ambient air temperature (T3), drying cabinet inlet (T1) and outlet (T2) temperatures, and temperature changes at the inlet - outlet points of the TES unit (T5, T6, T7, and T8) are given. The air circulating in the TES unit during the day provided the storage of thermal energy in the basalt stones. The temperature (T5) of the air circulating in the storage unit increased at the exit of the solar air collectors, and the air temperature (T6) decreased after transferring the thermal energy to the basalt stone. Thus, energy is stored in the basalt stone during the day. Since the TES unit was not activated in this drying study, the air at T7 and T8 points was stagnant and changed depending on the radiation value.

The daily radiation values (I), ambient air temperature (T3), inlet (T1), and outlet (T2) temperatures of the drying cabinet and the temperature changes at the inlet-outlet points of the TES unit (T5, T6, T7, T8) during the experiments carried out for the drying of 5 mm peach slices are given in Figure 3-b. Unlike Figure 3-a, in these trials, the TES unit was activated as of 17:30 and the thermal energy required for drying was obtained from the heat stored in the basalt stone. In the figure, the air temperature entering the drying cabinet (T1+T8) and the air temperatures (T2+T7) leaving the drying cabinet are shown with dashed lines for the active and de-active states of the TES unit. The change in the temperature of the air entering the drying cabinet when the TES unit is not used and the temperature change of the air entering the drying cabinet when the storage unit is active is shown in the circular active zone with dashed lines. When the active zone in the circle is examined, it is seen that the air at the desired temperature is supplied to the drying cabinet by using the storage system during the evening hours when the solar radiation values are very low. From the moment the TES unit was activated with the control of the dampers depending on the solar radiation, a sudden increase was observed in the T7 and T8 temperatures due to the energy taken from the basalt stone. Figure 3-c shows the temperatures in the drying of 10 mm thick peach slices using a TESDS. When the TES unit was not used, 10 mm thick peach samples were dried in two days, while when the storage unit was activated, they dried at 19:40. The fact that drying

continues even during hours when there is no solar radiation shortened the total drying time and enabled the desired dryness level to be reached more quickly.

In addition to the solar dryer, peach slices with 3-, 5- and 10-mm thicknesses were dried in a HPDS. Since it was not exposed to solar radiation, the system worked at constant temperature values. The system was set so that the temperature of the air entering the drying cabinet was 40 °C. Temperatures of 40-41 °C, 39-40 °C, 14 °C, 26 °C, and 26-27 °C were measured at T1, T2, T3, T4, and T5 points, respectively, in three drying experiments (Figure 1-b).

The time-dependent moisture content changes obtained from the experiments with three different drying methods are given in Figure 4. When the graph is examined, it is a natural result that as the thickness of the peach samples increases, the drying time is prolonged due to the high moisture content.

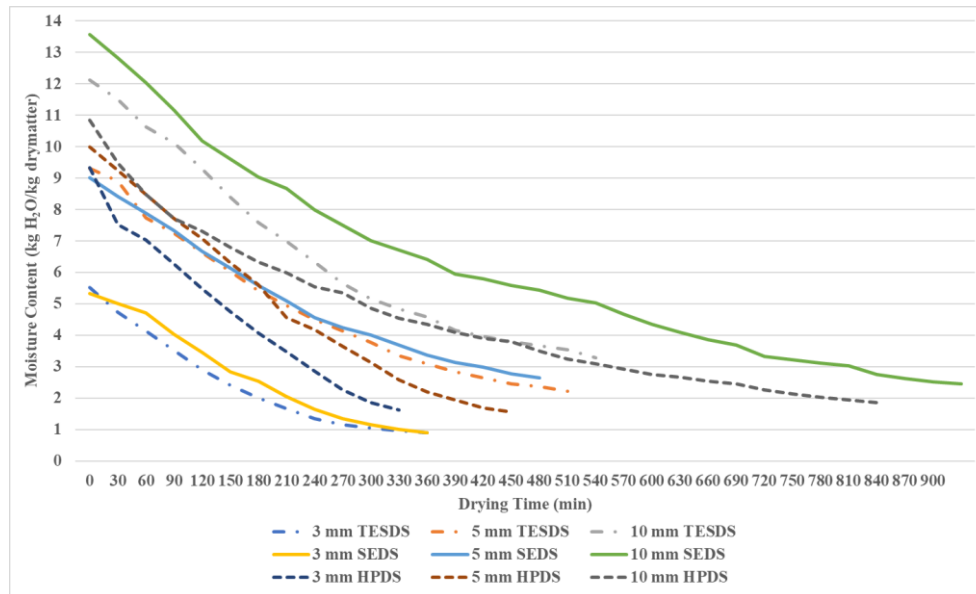


Figure 4-The time-dependent moisture content changes for experiments with three different drying methods

The most significant difference occurred during the drying of 10 mm thick peach samples. It has been observed that the drying studies performed with HPDS and SEDS are delayed to the second day, whereas in the drying performed with TESDS, the drying period ends at the end of the first day with the use of the heat stored during the day. It has been determined once again that the TESDS makes a positive contribution to the drying time.

The weight of the peach slices was measured in each experiment before and after drying, and the overall amount of moisture removed from the products was calculated. The drying system's electricity meter was used to calculate the consumption of electrical energy. For each experiment, the SMER, MER, and SEC values are shown in Table 3-a. In the 10 mm peach drying trials where the heat storage system was activated, it was observed that the MER value increased, and the SEC value decreased with the shortening of the drying time. On the other hand, in terms of the amount of moisture removed per unit of energy consumed, SEDS and TESDS systems seem to be quite successful compared to the heat pump drying system. It is seen that the highest energy consumption occurs with the heat pump drying system. Results similar to the SMER value range of 0.13 kg/kWh to 0.40 kg/kWh found in the study (Yahya et al. 2018) using a solar-assisted heat pump dryer were obtained.

Moisture content, water activity, color, and texture profile analyses of dried peach slices were made. Food analysis results for peach slices are given in Table 3-b. The moisture content of dried peach slices varies between 0.90 kg_{water}/kg_{drymatter} and 3.29 kg_{water}/kg_{drymatter}. When the drying methods were compared with each other, they were found to be statistically different ($P < 0.05$). Karaaslan et al., in their three different drying studies of peach in a solar dryer, found the final moisture content similar to our study (Karaaslan et al. 2021). Water activity has a direct relationship with equilibrium moisture content. As seen in Table 3-b, water activity results varied between 0.52 - 0.91. It was found that the water activity of 10 mm TESDS samples was the greatest and was significantly different from other samples ($P < 0.05$).

Color analyses of fresh and dried peaches were made, and the results were compared with each other. The color of peach slices before processing was determined as $L^* = 61.82 \pm 0.15$, $a^* = 15.09 \pm 0.07$, $b^* = 41.85 \pm 0.11$. L^* values, which indicate the lightness of the product, vary between 51.61 and 77.00. The L^* value of the 5 mm SEDS sample is very similar to that of fresh peach samples. The highest L^* values were obtained in products dried with a heat pump. When the a^* values were examined, it was seen that the products dried with solar energy turned red due to the browning that occurred during the drying process. The b^* values of the dried products varied between 34.03 - 56.33. The differences in L^* , a^* , and b^* values between the different

drying methods were found to be statistically significant ($P<0.05$). For each drying method, the increase in slice thickness and drying time caused a darkening in the product color, and L^* values decreased. The a^* and b^* values showed that the color change occurred mostly in yellow tones. Total color differences (ΔE) were calculated between 3.48 and 21.57. Minimum ΔE values were evaluated for 5 mm SEDS samples, and the highest ΔE values were evaluated for 5 mm HPDS samples. There was no significant change in ΔE values for 3 mm SEDS and 5 mm SEDS ($P>0.05$). In a study conducted in a solar dryer (García-Moreira et al. 2023), the color change values of peaches dried at different drying air speeds were found to be 13.28 ± 7.6 and 17.13 ± 4.4 . These results are especially similar to those from TESDS drying experiments. It was understood that the drying time due to the drying methods is effective on the color change value. The minimum ΔC was calculated for 3 mm SEDS.

The shear forces of fresh and dried peach slices were examined. Depending on the amount of drying and slice thickness, increases in shear force were observed. As can be seen from literature research, it has been revealed that food analysis results differ in peach drying studies (Tan et al. 2022). These differences between studies can be attributed to factors such as dryer type, drying time, drying temperature, and product type.

Table 3- a) Performance parameters of drying experiments and b) food analysis results of peach slices

<i>Performance parameters of drying experiments</i>								
	Dried Peach (g)	Consumed Energy (kW)	Evaporated Moisture (g)	MER (kg _w /h)	SMER (kg _w /kWh)	SEC (kWh/kg _w)	Drying Time (h)	
3 mm SEDS	2789.62	5.430	2344.90	0.39	0.43	2.32	6.00	
5 mm SEDS	3760.00	7.240	2895.13	0.35	0.40	2.50	8.16	
10 mm SEDS	6191.05	13.57	3901.47	0.26	0.29	3.44	14 (30.5)	
3 mm TESDS	2193.42	7.150	1817.24	0.29	0.25	4.00	6.16	
5 mm TESDS	3106.76	9.280	2538.04	0.32	0.27	3.70	8.00	
10 mm TESDS	5093.38	9.470	3359.92	0.41	0.35	2.85	8.16	
3mm HPDS	2310.92	9.548	1914.00	0.35	0.20	5.00	5.50	
5 mm HPDS	2490.28	12.60	2118.35	0.28	0.17	5.88	7.50	
10 mm HPDS	3048.00	24.64	2507.53	0.18	0.10	10.0	14.0	

<i>Food analysis results of peach slices</i>								
	Moisture content (kg _{water} /kg _{drymatter})	Water Activity (aw)	L^* (Brightness)	a^* (redness)	b^* (yellowness)	ΔE	ΔC	Shear Force (N)
Color values of fresh peach			61.82±0.15	15.09±0.07	41.85±0.11	0	0	2.94
3 mm SEDS	0.91±0.87 ^e	0.536±0.016 ^b	63.96±0.03 ^c	12.92±0.57 ^d	43.75±0.50 ^d	3.59±0.27 ^g	2.88±0.45 ^f	15.57
5 mm SEDS	2.64±0.55 ^b	0.522±0.102 ^b	60.33±0.13 ^f	16.38±0.16 ^c	38.98±0.20 ^e	3.48±0.27 ^g	3.14±0.15 ^f	43.86
10 mm SEDS	2.75±0.38 ^b	0.520±0.099 ^b	58.78±0.43 ^g	20.37±0.26 ^a	44.02±0.13 ^d	6.46±0.19 ^f	5.70±0.25 ^e	91.81
3 mm TESDS	0.90±0.37 ^e	0.639±0.024 ^b	74.54±0.19 ^c	16.81±0.67 ^{bc}	50.79±0.22 ^b	15.64±0.33 ^c	9.10±0.14 ^c	35.95
5 mm TESDS	2.23±0.27 ^c	0.659±0.007 ^b	57.55±0.28 ^h	20.43±0.22 ^a	34.03±0.09 ^f	10.38±0.41 ^e	9.45±0.33 ^c	86.83
10 mm TESDS	3.29±0.45 ^a	0.912±0.035 ^a	51.61±0.44 ⁱ	21.41±0.43 ^a	38.59±0.34 ^e	12.44±0.55 ^d	7.11±0.15 ^d	68.43
3mm HPDS	1.63±0.93 ^d	0.658±0.053 ^b	77.00±0.12 ^a	8.77±0.60 ^c	51.35±0.34 ^b	18.98±0.47 ^b	11.41±0.32 ^b	45.85
5 mm HPDS	1.56±0.37 ^d	0.659±0.006 ^b	75.48±0.27 ^b	7.66±0.35 ^c	49.73±0.20 ^c	21.57±0.44 ^a	10.83±0.26 ^b	40.63
10 mm HPDS	1.87±0.75 ^d	0.587±0.026 ^b	72.15±0.20 ^d	17.9±0.47 ^b	56.33±0.15 ^a	18.01±0.25 ^b	14.75±0.04 ^a	87.77

a - 1 Different letters within rows are significantly different ($P<0.05$)

4. Conclusions

Three different dryer types have been investigated in this study. Solar air-heated, solar with thermal energy storage, and heat-pump dryers were used to dry the peach slices. The heat storage unit loaded with basalt stone was put into operation for the continuity of drying during the hours when there is no daylight.

In the drying process using SEDS, the drying times of 3-, 5-, and 10-mm thicknesses were determined as 6, 8, and 14 hours, respectively. A 10 mm-thick peach slice was kept in the system for a total of 30.5 hours, and drying took place within 14 hours of this time. The remaining times passed as the period when drying was unavailable during the night. The drying was spread over two days. In the drying process with TESDS, the heat storage system was activated at the time when the solar radiation values were insufficient for drying. In 5- and 10-mm-thick peach slices, the drying air temperature increased with the heat taken from the heat storage system, and drying was carried out at low radiation values. In the dryer with a heat pump, drying times of 5.5, 7.5, and 14 hours were obtained, respectively, for all three thicknesses at constant drying temperatures.

Considering the amount of energy consumed, it is seen that the heat pump system consumes more energy than the solar energy system. The advantage of solar energy systems in terms of energy consumption has clearly emerged. In addition, the

drying time was shortened using the heat storage system, which resulted in savings in energy consumption. A decrease in SEC values was observed with the commissioning of the heat storage solar dryer.

This study not only demonstrates the effects of different dryer types on drying performance but also offers guidance on the use of thermal energy storage systems in drying applications. Drying food products of high quality in the shortest time with the lowest energy consumption should be the main target, and studies should be continuously improved in this direction.

Abbreviations

SEDS	Solar energy drying system
TESDS	Thermal energy storage drying system
HPDS	Heat pump drying system
SMER	Specific moisture extraction rate, kg _w /kWh
MER	Moisture extraction rate, kg _w /h
SEC	Specific energy consumption, kWh/kg _w
MoR	Moisture removed
EC	Energy consumed during drying
DT	Drying time
Nomenclature	
aw	Water activity
P	Vapor pressure of product, Pa
P ₀	Vapor pressure of pure water, Pa
L*	Brightness value
a*	Redness value
b*	Yellowness value
ΔE	Total color difference
ΔC	Color intensity

References

- Abubakar S, Umaru S, Kaisan M U, Umar U A, Ashok B & Nanthagopal K (2018). Development and performance comparison of mixed-mode solar crop dryers with and without thermal storage. *Renewable Energy* 128: 285–298. <https://doi.org/10.1016/j.renene.2018.05.049>
- Akin A, Gurlek G & Ozbalta N (2014). Mathematical model of solar drying characteristics for pepper (*Capsicum Annuum*). *Journal of Thermal Science and Technology* 34(2): 99-109
- Akpinar E K (2010). Drying of mint leaves in a solar dryer and under open sun: Modelling, performance analyses. *Energy Conversion and Management* 51(12): 2407–2418. <https://doi.org/10.1016/j.enconman.2010.05.005>
- Aktaş M, Koşan M, Çatalbaş C & Gök M (2019). Drying of Sliced Apple and Carrot with Heat Pump Technique: Performance Analysis (In Turkish). *Journal of Polytechnic* 22(3): 523-529. <https://doi.org/10.2339/politeknik.534443>
- Atalay H (2019). Comparative assessment of solar and heat pump dryers with regards to exergy and exergoeconomic performance. *Energy* 189: 116180. <https://doi.org/10.1016/j.energy.2019.116180>
- Atalay H (2020). Assessment of energy and cost analysis of packed bed and phase change material thermal energy storage systems for the solar energy-assisted drying process. *Solar Energy* 198: 124–138. <https://doi.org/10.1016/j.solener.2020.01.051>
- Ayyappan S, Mayilsamy K & Sreenarayanan V V (2016). Performance improvement studies in a solar greenhouse drier using sensible heat storage materials. *Heat and Mass Transfer* 52(3): 459–467. <https://doi.org/10.1007/s00231-015-1568-5>
- Baniasadi E, Ranjbar S & Boostanipour O (2017). Experimental investigation of the performance of a mixed-mode solar dryer with thermal energy storage. *Renewable Energy* 112: 143–150. <https://doi.org/10.1016/j.renene.2017.05.043>
- Baysal T, Ozbalta N, Gokbulut S, Capar B, Tastan O & Gurlek G (2015). Investigation of effects of various drying methods on the quality characteristics of apple slices and energy efficiency. *Journal of Thermal Science and Technology* 35(1): 135–144
- Bourdoux S, Li D, Rajkovic A, Devlieghere F & Uyttendaele M (2016). Performance of Drying Technologies to Ensure Microbial Safety of Dried Fruits and Vegetables. *Comprehensive Reviews in Food Science and Food Safety* 15(6): 1056-1066. <https://doi.org/10.1111/1541-4337.12224>
- Chaouch W B, Khellaf A, Mediani A, Slimani M E A, Loumani A & Hamid A (2018). Experimental investigation of an active direct and indirect solar dryer with sensible heat storage for camel meat drying in Saharan environment. *Solar Energy* 174: 328–341. <https://doi.org/10.1016/j.solener.2018.09.037>
- Fudholi A, Sopian K, Othman M Y & Ruslan M H (2014). Energy and exergy analyses of solar drying system of red seaweed. *Energy and Buildings* 68: 121–129. <https://doi.org/10.1016/j.enbuild.2013.07.072>
- Ganjehsarabi H, Dincer I & Gungor A (2014). Exergoeconomic Analysis of a Heat Pump Tumbler Dryer. *Drying Technology* 32(3): 352–360. <https://doi.org/10.1080/07373937.2013.829853>
- García-Moreira D P, Hernández-Guzmán H, Pacheco N, Cuevas-Bernardino J C, Herrera-Pool E, Moreno I & López-Vidaña E C (2023). Solar and Convective Drying: Modeling, Color, Texture, Total Phenolic Content, and Antioxidant Activity of Peach (*Prunus persica* (L.) Batsch) Slices. *Processes* 11(4): 1280. <https://doi.org/10.3390/pr11041280>

- Goh L J, Othman M Y, Mat S, Ruslan H & Sopian K (2011). Review of heat pump systems for drying application. *Renewable and Sustainable Energy Reviews* 15(9): 4788–4796. <https://doi.org/10.1016/j.rser.2011.07.072>
- Gunerhan H & Hepbasli A (2005). Utilization of Basalt Stone as a Sensible Heat Storage Material. *Energy Sources* 27(14): 1357–1366. <https://doi.org/10.1080/009083190523253>
- Gürlek G, Akdemir Ö & Güngör A (2015). Usage of Heat Pump Dryer in Food Drying Process and Apple Drying Application. *Pamukkale University Journal of Engineering Sciences* 21(9): 398–403. <https://doi.org/10.5505/pajes.2015.35761>
- Gürlek G, Özbalta N & Güngör A (2009). Solar tunnel drying characteristics and mathematical modelling of tomato. *Journal of Thermal Science and Technology* 29(1): 15–23
- Hartlieb P, Toifl M, Kuchar F, Meisels R & Antretter T (2016). Thermo-physical properties of selected hard rocks and their relation to microwave-assisted comminution. *Minerals Engineering* 91: 34–41. <https://doi.org/10.1016/j.mineng.2015.11.008>
- Hepbasli A, Colak N, Hancioglu E, Icier F & Erbay Z (2010). Exergoeconomic Analysis of Plum Drying in a Heat Pump Conveyor Dryer. *Drying Technology* 28(12): 1385–1395. <https://doi.org/10.1080/07373937.2010.482843>
- Huang L, Zhang M, Mujumdar A S & Lim R (2011). Comparison of four drying methods for re-structured mixed potato with apple chips. *Journal of Food Engineering* 103(3): 279–284. <https://doi.org/10.1016/j.jfoodeng.2010.10.025>
- Kant K, Shukla A, Sharma A, Kumar A & Jain A (2016). Thermal energy storage based solar drying systems: A review. *Innovative Food Science & Emerging Technologies* 34: 86–99. <https://doi.org/10.1016/j.ifset.2016.01.007>
- Karaaslan S, Ekinci K, Ertekin C & Kumbul B S (2021). Thin layer peach drying in solar tunnel drier. *Erwerbs-Obstbau* 63(1): 65–73. <https://doi.org/10.1007/s10341-020-00536-4>
- Kohli D, Champawat P S, Jain S K, Mudgal V D & Shahi N C (2021). Mathematical modelling for drying kinetics of asparagus roots (*Asparagus Racemosus* L.) and determination of energy consumption. *Biointerface Research in Applied Chemistry* 12(3): 3572–3589. <https://doi.org/10.33263/BRIAC123.35723589>
- Lee J H & Kim H J (2009). Vacuum drying kinetics of Asian white radish (*Raphanus sativus* L.) slices. *LWT - Food Science and Technology* 42(1): 180–186. <https://doi.org/10.1016/j.lwt.2008.05.017>
- Liu M, Wang S, Liu R & Yan J (2019). Energy, exergy and economic analyses on heat pump drying of lignite. *Drying Technology* 37(13): 1688–1703. <https://doi.org/10.1080/07373937.2018.1531883>
- Mirzabeigi Kesbi O, Sadeghi M & Mireei S A (2016). Quality assessment and modeling of microwave-convective drying of lemon slices. *Engineering in Agriculture, Environment and Food* 9(3): 216–223. <https://doi.org/10.1016/j.eaef.2015.12.003>
- Nahhas T, Py X & Sadiki N (2019). Experimental investigation of basalt rocks as storage material for high-temperature concentrated solar power plants. *Renewable and Sustainable Energy Reviews* 110: 226–235. <https://doi.org/10.1016/j.rser.2019.04.060>
- Nakilcioğlu-Taş E & Ötleş S (2018). Colour change kinetics of the inner and outer surface of brussels sprouts during microwave drying process. *Journal of Agricultural Sciences* 24(4): 488–500.
- Natarajan K, Thokchom S S, Verma T N & Nashine P (2017). Convective solar drying of *Vitis vinifera* & *Momordica charantia* using thermal storage materials. *Renewable Energy* 113: 1193–1200. <https://doi.org/10.1016/j.renene.2017.06.096>
- Nindo C I, Sun T, Wang S W, Tang J & Powers J R (2003). Evaluation of drying technologies for retention of physical quality and antioxidants in asparagus (*Asparagus officinalis*, L.). *LWT - Food Science and Technology* 36(5): 507–516. [https://doi.org/10.1016/S0023-6438\(03\)00046-X](https://doi.org/10.1016/S0023-6438(03)00046-X)
- Orikasa T, Wu L, Shiina T & Tagawa A (2008). Drying characteristics of kiwifruit during hot air drying. *Journal of Food Engineering* 85(2): 303–308. <https://doi.org/10.1016/j.jfoodeng.2007.07.005>
- Polat A, Taşkin O & İzli N (2021). Application of drying techniques on peach puree. *Tarım Bilimleri Dergisi* <https://doi.org/10.15832/ankutbd.595857>
- Qiu Y, Li M, Hassanien R H E, Wang Y, Luo X & Yu Q (2016). Performance and operation mode analysis of a heat recovery and thermal storage solar-assisted heat pump drying system. *Solar Energy* 137: 225–235. <https://doi.org/10.1016/j.solener.2016.08.016>
- Queiroz R, Gabas A L & Telis V R N (2004). Drying kinetics of tomato by using electric resistance and heat pump dryers. *Drying Technology* 22(7): 1603–1620. <https://doi.org/10.1081/DRT-200025614>
- Rehman H U, Naseer F & Ali H M (2023). An experimental case study of solar food dryer with thermal storage using phase change material. *Case Studies in Thermal Engineering* 51: 103611. <https://doi.org/10.1016/j.csite.2023.103611>
- Saidani F, Giménez R, Aubert C, Chalot G, Betrán J A & Gogorcena Y (2017). Phenolic, sugar and acid profiles and the antioxidant composition in the peel and pulp of peach fruits. *Journal of Food Composition and Analysis* 62: 126–133. <https://doi.org/10.1016/j.jfca.2017.04.015>
- Şevik S, Aktaş M, Dolgun E C, Arslan E & Tuncer A D (2019). Performance analysis of solar and solar-infrared dryer of mint and apple slices using energy-exergy methodology. *Solar Energy* 180: 537–549. <https://doi.org/10.1016/j.solener.2019.01.049>
- Singh D, Mishra S & Shankar R (2022). Drying kinetics and performance analysis of indirect solar dryer integrated with thermal energy storage material for drying of wheat seeds: an experimental approach. *Energy Sources, Part A: Recovery, Utilization, and Environmental Effects* 44(3): 7967–7985. <https://doi.org/10.1080/15567036.2022.2118907>
- Tan S, Miao Y, Zhou C, Luo Y, Lin Z, Xie R & Li W (2022). Effects of hot air drying on drying kinetics and anthocyanin degradation of blood-flesh peach. *Foods* 11(11): 1596. <https://doi.org/10.3390/foods11111596>
- Vijayan S, Arjunan T V & Kumar A (2020). Exergo-environmental analysis of an indirect forced convection solar dryer for drying bitter gourd slices. *Renewable Energy* 146: 2210–2223. <https://doi.org/10.1016/j.renene.2019.08.066>
- Yahya M, Fahmi H, Fudholi A & Sopian K (2018). Performance and economic analyses on solar-assisted heat pump fluidised bed dryer integrated with biomass furnace for rice drying. *Solar Energy* 174: 1058–1067. <https://doi.org/10.1016/j.solener.2018.10.002>

